Nanoscale

PAPER

View Article Online
View Journal | View Issue

Cite this: *Nanoscale*, 2019, **11**, 21867

Exciton–phonon interaction in quasi-two dimensional layered $(PEA)_2(CsPbBr_3)_{n-1}PbBr_4$ perovskite†

Hao Long, *[a] Xiang Peng,[a] Jianxun Lu,[b] Kebin Lin,[b] Liqiang Xie,[b] Baoping Zhang,[a] Leiying Ying[a] and Zhanhua Wei *[b]

Two-dimensional (2D) Ruddlesden-Popper perovskites with bulky organic cations have attracted extensive attention in light-emitting devices and photovoltaics due to their robust environment stability, tunable luminescent color, strong exciton binding and promising efficiency. A quantum well (QW) structure is spontaneously formed by sandwiching $PbBr_4$ layers into bulky organic cations. However, some intrinsic excitonic mechanisms in these materials still need to be elucidated. In this study, the exciton–phonon interaction of quasi-2D $(PEA)_2(CsPbBr_3)_{n-1}PbBr_4$ with different $PbBr_4$ layer numbers (n) was analyzed by temperature-varied photoluminescence (PL), scanning electron microscopy (SEM) and powder X-ray diffraction (PXRD). The mechanism of bandgap shifting with temperature was found to be dominated by the thermal expansion effect in the large-n 2D and bulk perovskite, and gradually switched to exciton–phonon interaction in the n = 1 $(PEA)_2PbBr_4$ phase, indicating enhanced exciton–phonon interaction in the thinner quantum well structure. Further analysis showed that the enhanced exciton–phonon interaction originated from the longitudinal optical phonon-exciton Fröhlich interaction rather than acoustic phonon-exciton coupling. We believe that our results will benefit the further optimization of light-emitting devices based on 2D perovskites.

Received 9th August 2019,
Accepted 24th October 2019

DOI: 10.1039/c9nr06834a

rsc.li/nanoscale

1. Introduction

Although metal halide perovskites have achieved astonishing progress in photovoltaic and light-emitting efficiency, to date, they have not yet overcome the environmental durability for industrial applications.[1–4] Recently, 2D perovskites have attracted increasing interest in virtue of their outstanding environmental benignity and excellent electronic merits for light-emitting devices (LEDs), laser diodes (LDs), solar cells and other promising applications.[5,6] Typically, 2D perovskite materials have a general formula of $L_2(APbX_3)_{n-1}PbX_4$ with L = bulky organic cation as a barrier spacer; A = cations (*e.g.*, Cs, Rb, methylamine (MA)) and X = halogen anions. These materials form artificial quantum well structures with n layers of PbX_4 as well regions sandwiched by bulky organic spacers. The layer number n significantly influences the optical and electronic properties of these material systems (including exciton binding energy and mobility).[7] Strong dielectric and quantum confinement effects enable stable excitons at room temperature. The efficiencies of solar cells and LEDs based on 2D perovskites have achieved 17.4%[8] and 14.36%,[9] respectively. However, the intrinsic luminescence mechanisms in these 2D material systems still need to be disclosed. In this work, the exciton–phonon interaction of the $(PEA)_2(CsPbBr_3)_{n-1}PbBr_4$ material (PEA: 2-phenylethylamine) with different layer number n was investigated. The intrinsic mechanisms in the exciton–phonon coupling causing the bandgap shifting and spectrum broadening were analyzed.

2. Experimental

$CsPbBr_3$ and PEABr in a 1 : 1 molar ratio were dissolved in a dimethyl sulfoxide (DMSO) solution. Then, quasi-2D $(PEA)_2(CsPbBr_3)_{n-1}PbBr_4$ thin film was formed on a quartz substrate by the one-step spin coating method. Owing to the non-uniform distribution ratio of PEABr : $CsPbBr_3$, mixed phase quasi-2D $(PEA)_2(CsPbBr_3)_{n-1}PbBr_4$ materials with various n values were simultaneously synthesized on a single

[a]*School of Electronic Science and Engineering (National Model Microelectronics College), Xiamen University, Xiamen 361005, People's Republic of China. E-mail: longhao@xmu.edu.cn*
[b]*Engineering Research Center of Environment-Friendly Functional Materials, Ministry of Education, College of Materials Science & Engineering, Huaqiao University, Xiamen, People's Republic of China. E-mail: weizhanhua@hqu.edu.cn*

†Electronic supplementary information (ESI) available. See DOI: 10.1039/c9nr06834a

substrate. SEM images were taken by ZEISS instruments. PXRD was performed with a 2θ value between 4° to 20°. The temperature-dependent PL measurement was conducted under a temperature range from 50 K to 300 K with a 275 μW, 325 nm continuous-wave He–Cd laser excitation source. For comparison, pure phase 2D $(PEA)_2PbBr_4$ was also fabricated and studied.

3. Results and discussion

The SEM images in Fig. 1(a) shows the full coverage of the perovskite thin film with excellent surface uniformity, which benefits the fabrication of the thin film devices. In addition, this thin film was characterized as crystal 'flakes' with a typical size of 50 nm–200 nm (Fig. 1(b)). This flake morphology with crystal sizes ranging in hundreds of nanometers plausibly originated from the quantum well structures of the 2D layers observed from the crystallography.

A series of low angle PXRD peaks were detected by the 2θ scan, as shown in Fig. S1a.† In addition to the pure phase 2D $(PEA)_2PbBr_4$ (Fig. S1b†), the PXRD results showed clear diffraction modes at about 5°, 11°, and 16°, which originated from the (002), (004) and (006) crystal planes of the $PbBr_4$ octahedrons,[10] and was direct proof of the 2D structure formation in our samples.

Room temperature absorption and PL measurements were also taken, showing various excitonic peaks in agreement with the observed different layered quasi-2D perovskite (Fig. 2). The absorption spectrum exhibited four excitonic peaks superimposed on the absorption edge. The four bands were ascribed with the $n = 1$ to $n = 4$ layers of $(PEA)_2(CsPbBr_3)_{n-1}PbBr_4$ since the exciton energy decreased monotonously with increasing layer number.[11] In the PL spectrum, four anomalous peaks appeared near the exciton positions in the absorption spectrum, and all peaks showed a red Stokes shift. The Stokes shifts of these peaks ranged from 20 meV to 34 meV, which were caused by the inhomogeneous broadening and funneling effects.[12] In addition, a peak located at 515 nm appeared in the PL spectrum, which was absent in the absorption spectrum. This luminescent band originated from the bulk $CsPbBr_3$ material. Identical PL bands have been extensively

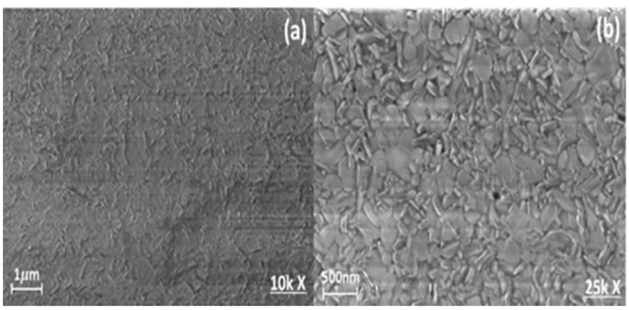

Fig. 1 SEM images of quasi-2D $(PEA)_2(CsPbBr_3)_{n-1}PbBr_4$ perovskite: (a) low magification shows uniform coverage; (b) large magnification shows nano-sized flakes.

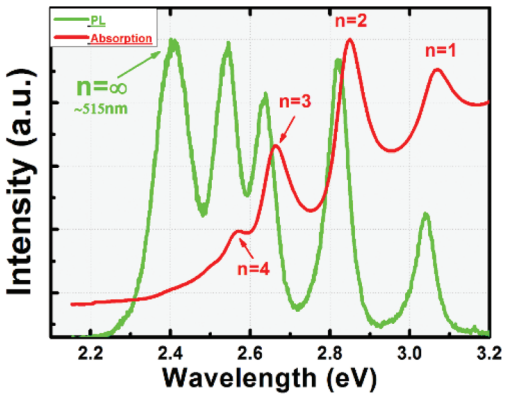

Fig. 2 RT absorption and PL spectra of 2D $(PEA)_2(CsPbBr_3)_{n-1}PbBr_4$ show multiple excitonic bands.

proved by our previous work and also by other groups.[13,14] The reason for the absence of the 515 nm band in the absorption may be the low density of states in the bulk $CsPbBr_3$ exciton energy levels.

Due to the robust exciton binding characteristic and also fast recombination rate (Fig. S2†), the distinctive excitonic luminescence bands from $n = 1$ to 4 and bulk $(PEA)_2(CsPbBr_3)_{n-1}PbBr_4$ survived from 50 K to 300 K, as shown in Fig. 3. The evolution of the PL spectra with temperature revealed the fundamental properties of the excitons in this material.

First, the semiconductor bandgap will change with temperature, inducing peak shifts in the PL spectra. The bandgap (E_g) evolution of the semiconductors is under a joint influence of two main mechanisms, including the thermal expansion effect and exciton–phonon interactions, which is expressed by:[15]

$$\frac{dE_g}{dT} = \frac{\partial E_g}{\partial V}\frac{\partial V}{\partial T} + \sum_{i,q}\left(\frac{\partial E_g}{\partial n_{i,q}}\right)\left(n_{i,q} + \frac{1}{2}\right). \quad (1)$$

In the first term, the temperature expands the lattices, leading to the bandgap blue-shift by $\frac{\partial E_g}{\partial V}\frac{\partial V}{\partial T}$, where V is the

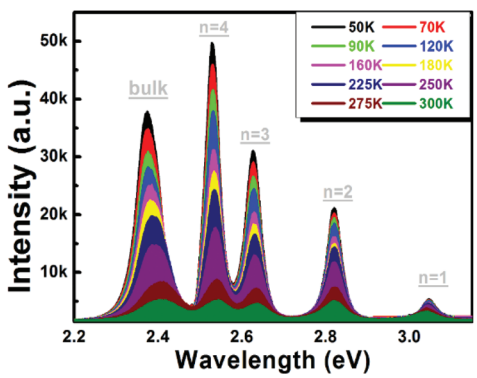

Fig. 3 Temperature dependence of the PL spectra from 50 K to 300 K.

solid volume.[16] In the second term of the exciton–phonon interaction, the bandgap was red-shifted by $\sum_{i,q}\left(\frac{\partial E_g}{\partial n_{i,q}}\right)\times\left(n_{i,q}+\frac{1}{2}\right)$, where $n_{i,q}=\frac{1}{\exp\left(\frac{\hbar\omega_{i,q}}{k_B T}\right)-1}$ is the phonon numbers of the i_{th} branch and q is the wave number, $\hbar\omega_{i,q}$ is the phonon energy, and k_B is the Boltzmann constant.[16,17] The coefficient $\frac{\partial E_g}{\partial n_{i,q}}$ by phonon number is always treated as a negative constant. Typically, the contribution of thermal expansion could approximately be negligible in conventional semiconductors (*e.g.*, GaAs, GaN, Si); thus, the exciton–phonon interaction will induce the normal redshift of the bandgap with temperature.[18] However, in the peculiar lead-based perovskite system, the thermal expansion effect was eminent and competed with the exciton–phonon interaction. Many bulk perovskite materials exhibited a blueshift when the temperature increased.[16,17]

In our experiments, as shown in Fig. 4, the luminescence peaks of $(PEA)_2(CsPbBr_3)_{n-1}PbBr_4$ with different n featured different evolution tendencies by temperature. Bulk $CsPbBr_3$ with $n = \infty$ was almost linearly blueshifted with temperature with a slope of about 0.083 meV K^{-1}, which demonstrates the domination of the thermal expansion effect rather than exciton–phonon interaction in this material. This result coincided well with previous results in the bulk perovskite.[14] In addition, the blueshift slope decreased when the layer number decreased, with 0.032 meV K^{-1} of $n = 4$, 0.015 meV K^{-1} of $n = 3$ and 0.002 meV K^{-1} of $n = 2$. Interestingly, in the $n = 1$ $(PEA)_2PbBr_4$ with only a single-layered $PbBr_4$ octahedron sandwiched by PEA organic material, the luminescent peak was redshifted with temperature. This gradual switching of the PL peak evolution from a blueshift to redshift revealed not only the suppression of the thermal expansion effects, but also the gradual enhancement of the exciton–phonon interactions with decreasing n in the quasi-2D $(PEA)_2(CsPbBr_3)_{n-1}PbBr_4$ materials. The suppression of thermal expansion in the low-dimension perovskite could be explained by the compression effect of the bulky PEA cation to the $PbBr_4$ octahedron. The enhancement of the exciton–phonon coupling in the low-dimensional perovskite was also reported in $(BA)_2(MA)_{n-1}PbnI_{3n+1}$[19,20] (BA = $C_4H_9NH_3$), exfoliated (PEA) $PbBr_4$,[10] $(PEA)_2PbCl_4$,[21] and $(PEA)_2(MA)_{n-1}[Pb_nI_{3n+1}]$.[22] This phenomenon should be related with the different excitonic confinement strengths of different n phases in the quasi-2D perovskite. On gradually thinning the QW layers, excitons would be strongly restricted in the $PbBr_4$ octahedron and increase the coupling strength with the phonons inside.[23] Our results were also in line with I. V. Bondarev's theoretical calculation, who anticipated that the exciton–phonon scattering will be significantly enhanced by exciton restriction.[24] It should be noted that although many works reported that the exciton–phonon interaction was enhanced by decreasing the layer number n, the effects on the peak shifts and PL broadening were significantly different. In $(BA)_2(MA)_{n-1}PbnI_{3n+1}$[19,20] and $(PEA)_2(MA)_{n-1}[Pb_nI_{3n+1}]$,[22] the phase transition occurred at a low temperature. The blueshift of the PL peaks existed throughout the PL spectra from low temperatures to 300 K. $(PEA)_2PbCl_4$[21] showed very broad self-trapped exciton emission and upconversion properties. To further analyze the intrinsic origination of the enhancement of the exciton–phonon interaction in the quasi-2D perovskite, the line width dependences on temperature need to be investigated.

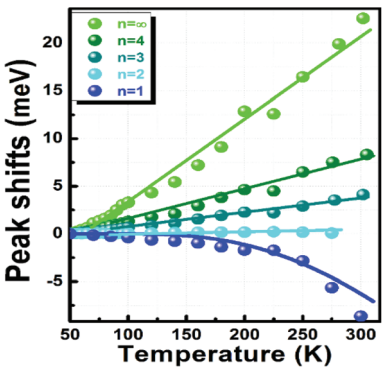

Fig. 4 The PL peak dependence on temperature switched from blueshift to redshift by decreasing the layer number n.

In general, the exciton–phonon interaction includes two sources: an acoustic (AC) phonon deformation scattering and a longitudinal optical (LO) phonon Fröhlich interaction.

In Fig. 5, all the line widths of $(PEA)_2(CsPbBr_3)_{n-1}PbBr_4$ with various n layer numbers exhibited notable superimposition characteristics of linear increasing in the low temperature regime (50 K–200 K) and a super-linear dependence in the high temperature regime (>200 K). Since the energy of the acoustic phonon was typically low (<10 meV), the line width always broadened linearly with increasing temperature when the acoustic phonon scattering dominated. Conversely, if the LO phonon Fröhlich interaction dominated, then the super-linear temperature dependence of the line width appeared due to the higher energy of the LO phonon (typically >20 meV). In our case, at low temperature, the LO phonon was inactive due to its large vibration energy. Thus, the acoustic phonon scattering dominated, rendering the linear width broadening. With increasing temperature, the LO phonons were gradually thermally activated. The interaction between the LO phonon and exciton switched the width-broadening into the super-linear regime. The line widths were fitted by eqn (2):[25,26]

$$\Gamma(T)=\Gamma_0+\Gamma_{ac}T+\frac{\Gamma_{op}}{\left(\exp\left(\frac{E_{op}}{k_B T}\right)-1\right)} \quad (2)$$

where Γ_0 is the inhomogeneous broadening and Γ_{ac} is the acoustic phonon coupling coefficient. Γ_{op} and E_{op} are the LO phonon coupling coefficient and average LO phonon energy, respectively. In Fig. 5f, the coupling strength between the LO phonon and exciton increased monotonously when the layer numbers were decreased. This could be explained by the stron-

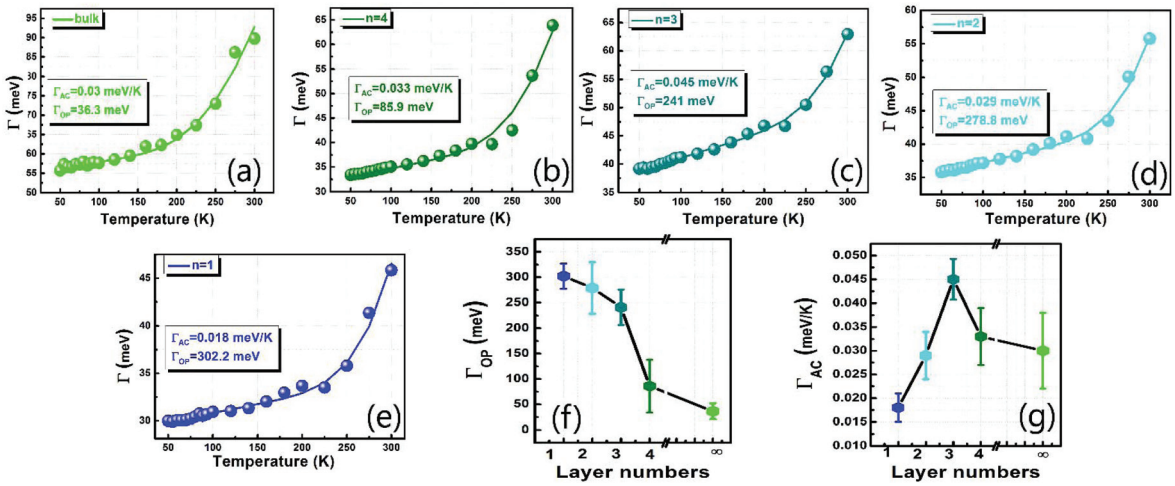

Fig. 5 (a–e) Width broadening with temperature of $(PEA)_2(CsPbBr_3)_{n-1}PbBr_4$ with different n values; and (f and g) LO phonon-exciton and acoustic phonon coupling strength dependence on the layer numbers of $PbBr_4$.

ger confinement of the exciton in the thinner QW structures, which was supported by the intensity dependence on temperature (Fig. S3†). The exciton binding energy of the n = 1 layer fitted from intensity quenching was 129.9 meV, which was much larger than the binding energy (67.9 meV) of the bulk $CsPbBr_3$ material. The 302 meV energy value of Γ_{op} of n = 1 in the quasi-2D materials was in line with that reported in the literature.[10,20,21] This is larger than the binding energy (163 meV) of pure phase $(PEA)_2PbBr_4$ (Fig. S4†), which could be understood by the lateral confinement of the exciton in the nano-sized flakes in the quasi-2D material as shown in the SEM images (Fig. 1b). In addition, the acoustic phonon-exciton coupling strength arrived at a maximum value at the n = 3 layer in Fig. 5g. The acoustic phonon demonstrates the vibrations of the mass center of the unit cells. As discussed above, sandwiching the $PbBr_4$ quantum well layers will suppress the vertical vibration of the $PbBr_4$ octahedron. The acoustic phonon vibration could be restricted by decreasing the layer number. However, the LO phonon would not be influenced, since the LO phonon is representative of the lateral vibration of the atoms. Therefore, it could be concluded that the enhanced exciton–phonon interaction resulting in the bandgap redshift in the n = 1 $(PEA)_2(CsPbBr_3)_{n-1}PbBr_4$ perovskite was ascribed to the increased LO phonon-exciton Fröhlich interactions.

4. Conclusions

In summary, the PL spectral temperature dependence of the quasi-2D perovskite $(PEA)_2(CsPbBr_3)_{n-1}PbBr_4$ with n = 1, 2, 3, 4 and ∞ and the pure phase $(PEA)_2PbBr_4$ materials were analyzed. The bandgap dependence of the quasi-2D layered perovskites switched from a blueshift to redshift from n = ∞ to n = 1, showing the gradual increasing of the exciton–phonon coupling. Further analysis of the PL width broadening demonstrated that the LO phonon-exciton Fröhlich interactions dominated the increased exciton–phonon coupling in the low-dimensional perovskites. We believe that our results will benefit the further optimization of light-emitting devices based on 2D perovskites.

Conflicts of interest

There are no conflicts to declare.

Acknowledgements

The project was supported by the National Natural Science Foundation of China (61704140, 51802102 and 21805101), the Natural Science Foundation of Fujian Province of China (No. 2019J05023), the Fundamental Research Funds for the Central Universities (ZQN-PY607) and Scientific Research Funds of Huaqiao University (16BS201, 17BS409 and 19BS105).

References

1 K. B. Lin, J. Xing, L. N. Quan, F. Arquer, X. W. Gong, J. X. Lu, L. Q. Xie, W. J. Zhao, D. Zhang, C. Z. Yan, W. Q. Li, X. Y. Liu, Y. Lu, J. Kirman, E. H. Sargent, Q. H. Xiong and Z. H. Wei, *Nature*, 2018, **562**, 245–248.
2 C. C. Stoumpos and M. G. Kanatzidis, *Acc. Chem. Res.*, 2015, **48**, 2791–2802.
3 B. R. Sutherland and E. H. Sargent, *Nat. Photonics*, 2016, **10**, 295–302.
4 S. A. Veldhuis, P. P. Boix, N. Yantara, M. J. Li, T. C. Sum, N. Mathews and S. G. Mhaisalkar, *Adv. Mater.*, 2016, **28**, 6804–6834.
5 S. Silver, Q. Dai, H. Li and J.-L. Brédas, *Adv. Energy Mater.*, 2019, 1901005.

6 H. Lai, B. Kan, T. Liu, N. Zheng, Z. Xie, T. Zhou, X. Wan, X. Zhang, Y. Liu and Y. Chen, *J. Am. Chem. Soc.*, 2018, **140**, 11639.
7 Y. Zheng, T. Niu, X. Ran, J. Qiu, B. Li, Y. Xia, Y. Chen and W. Huang, *J. Mater. Chem. A*, 2019, **7**(23), 13860–13872.
8 H. Zheng, G. Liu, L. Zhu, J. Ye, X. Zhang, A. Alsaedi, T. Hayat, X. Pan and S. Dai, *Adv. Energy Mater.*, 2018, **8**, 1800051.
9 X. Yang, X. Zhang, J. Deng, Z. Chu, Q. Jiang, J. Meng, P. Wang, L. Zhang, Z. Yin and J. You, *Nat. Commun.*, 2018, **9**, 570.
10 Y. Liang, Q. Shang, Q. Wei, L. Zhao, Z. Liu, J. Shi, Y. Zhong, J. Chen, Y. Gao, M. Li, *et al.*, *Adv. Mater.*, 2019, 1903030.
11 Y. Fu, W. Zheng, X. Wang, M. P. Hautzinger, D. Pan, L. Dang, J. C. Wright, A. Pan and S. Jin, *J. Am. Chem. Soc.*, 2018, **140**(46), 15675–15683.
12 M. Yuan, L. N. Quan, R. Comin, G. Walters, R. Sabatini, O. Voznyy, S. Hoogland, Y. Zhao, E. M. Beauregard, P. Kanjanaboos, *et al.*, *Nat. Nanotechnol.*, 2016, **11**(10), 872–877.
13 Z. H. Wei, A. Perumal, R. Su, S. Sushant, J. Xing, Q. Zhang, S. T. Tan, H. V. Demir and Q. H. Xiong, *Nanoscale*, 2016, **8**, 18021.
14 H. Long, X. Peng, K. Lin, L. Xie, J. Lu, B. Zhang, L. Ying and Z. Wei, *Appl. Phys. Express*, 2019, **12**(5), 052003.
15 C. Yu, Z. Chen, J. J. Wang, W. Pfenninger, N. Vockic, J. T. Kenney and K. Shum, *J. Appl. Phys.*, 2011, **110**(6), 63526.
16 M. Sebastian, J. A. Peters, C. C. Stoumpos, J. Im, S. S. Kostina, Z. Liu, M. G. Kanatzidis, A. J. Freeman and B. W. Wessels, *Phys. Rev. B: Condens. Matter Mater. Phys.*, 2015, **92**, 235210.
17 K. Wei, Z. J. Xu, R. Chen, X. Zheng, X. G. Cheng and T. Jiang, *Opt. Lett.*, 2016, **41**, 16.
18 S. Chichibu, T. Azuhata, T. Sota and S. Nakamura, *J. Appl. Phys.*, 1996, **79**, 2784.
19 S. Wang, J. Ma, W. Li, J. Wang, H. Wang, H. Shen, J. Li, J. Wang, H. Luo and D. Li, *J. Phys. Chem. Lett.*, 2019, 2546–2553.
20 L. Ni, U. Huynh, A. Cheminal, T. H. Thomas, R. Shivanna, T. F. Hinrichsen, S. Ahmad, A. Sadhanala and A. Rao, *ACS Nano*, 2017, **11**(11), 10834–10843.
21 P. Cai, Y. Huang and H. J. Seo, *J. Phys. Chem. Lett.*, 2019, 4095–4102.
22 Y. Zhang, R. Wang, Y. Li, Z. Wang, S. Hu, X. Yan, Y. Zhai, C. Zhang and C. Sheng, *J. Phys. Chem. Lett.*, 2019, **10**(1), 13–19.
23 K. Thirumal, W. K. Chong, W. Xie, R. Ganguly, S. K. Muduli, M. Sherburne, M. Asta, S. Mhaisalkar, T. C. Sum, H. S. Soo, *et al.*, *Chem. Mater.*, 2017, **29**, 3947–3953.
24 I. V. Bondarev, S. A. Maksimenko and G. Y. Slepyan, *Phys. Rev. B: Condens. Matter Mater. Phys.*, 2003, **68**, 073310.
25 K. Wu, A. Bera, C. Ma, Y. Du, Y. Yang, L. Li and T. Wu, *Phys. Chem. Chem. Phys.*, 2014, **16**, 22476–22481.
26 Z. Liu, Q. Shang, C. Li, L. Zhao, Y. Gao, Q. Li, J. Chen, S. Zhang, X. Liu, Y. Fu, *et al.*, *Appl. Phys. Lett.*, 2019, **114**(10), 101902.